Article

Comparative Performance of Exchange and Correlation Density Functionals in Determining Intermolecular Interaction Potentials of the Methane Dimer

Sheng D. Chao, and Arvin Huang-Te Li

J. Phys. Chem. A, **2007**, 111 (38), 9586-9590 • DOI: 10.1021/jp074052n

Comparative Performance of Exchange and Correlation Density Functionals in Determining Intermolecular Interaction Potentials of the Methane Dimer†

Sheng D. Chao* and Arvin Huang-Te Li

Institute of Applied Mechanics, National Taiwan University, Taipei 106, Taiwan ROC

Received: May 25, 2007

We have calculated the interaction potentials of the methane dimer for the minimum-energy D_{3d} conformation using the density functional theory (DFT) with 90 density functionals chosen from the combinations of nine exchange and 10 correlation functionals. Several hybrid functionals are also considered. While the performance of an exchange functional is related to the large reduced density gradient of the exchange enhancement factor, the correlation energy is determined by the low-density behavior of a correlation enhancement factor. Our calculations demonstrate that the correlation counterpart plays an equally important role as the exchange functional in determining the van der Waals interactions of the methane dimer. These observations can be utilized to better understand the seemingly unsystematic DFT interaction potentials for weakly bound systems.

Introduction

van der Waals complexes constitute an important intermediate between free molecules and a condensed liquid and play a crucial role in the condensation and evaporation processes in phase transitions. Besides, packing, assembling, and cohesion of weakly bound biomolecular complexes such as DNA and protein into stable and functionalized conformations are gauged by specific van der Waals interactions.[1−3] A detailed investigation of these interactions provides much insight into important dynamic processes in molecular physics, solution chemistry, and structural biology. Experimental studies of van der Waals molecules abound but have been plagued with incomplete sampling of the potential energy surfaces.[4−5] Quantum chemistry calculations serve as a complementary way with experiments to investigate these illusive but important interactions.[6−9]

In the wave function based theory, van der Waals attractions are due to the correlation effect that is not included in the Hartree−Fock (HF) self-consistent method. Usually a high-level post-HF theory (such as the Møller−Plesset perturbation theory[10] or the coupled cluster theory[11]) and a large basis set are required to obtain a binding energy with a chemical accuracy of, say, 0.1 kcal/mol. Unfortunately, computational costs of these methods scale nonlinearly with respect to the number of basis functions (to the power of 5 or higher), which quickly reach the limit of current computing power.[12] Kohn−Sham density functional theory (KS−DFT)[13] provides an appealing alternative to the wave function based electronic structure theory due to its possibility to obtain equally accurate results with much less computational costs. KS−DFT has been successful in producing the geometry and energetics of extended systems and occasionally even for atoms and molecules. However, KS−DFT using the local density approximation (LDA) or generalized gradient approximation (GGA) functionals, being applied to weakly bound systems, often yields unsystematic results or spurious convergence behaviors that were poorly understood.[14−16] It is often found that the conclusions drawn from the study of a specific system cannot be universally applied to other systems. Definitely there are error cancellations between the exchange and the correlation functionals. Therefore, the relative performance of the exchange and correlation functionals should be investigated separately. Besides, semilocal GGA functionals have intrinsic limitation in modeling the correlation effect. As a matter of fact, there are two components of the correlation effect. The dynamic correlation is important in short and medium ranges of interaction, while the static (or nondynamic, near-degeneracy, or sometimes left−right) correlation dominates the long-range part.[17−18] Lack of the nonlocal static correlation in the LDA and GGA functionals is believed to be responsible for the deficiency of using DFT to obtain the long-range van der Waals interactions. In particular, it has been known that DFT using semilocal functionals cannot obtain the correct asymptotic long-range potential tail. However, improved GGA and meta-GGA functionals do contain some dynamic correlation that is important in short-range interactions.[19] Therefore, one expects the applicability of modern GGA and meta-GGA functionals in determining the equilibrium properties (such as the bond length and the binding energy) of van der Waals molecules.

Many previous theoretical studies put much emphasis on the performance of an exchange functional. In calculations of the electronic properties of atoms and molecules, the correlation energy contributes only 10% or less to the total energies.[20] It is found that the exchange energy can be related to the large reduced density gradient, $s = (|\nabla\rho|)/(2(3\pi^2)^{1/3}\rho^{4/3})$, ρ being the density, of the GGA exchange enhancement factor.[21] However, for van der Waals interactions, a large s actually means a low density because the electron overlapping is relatively small. Because correlation energy could be significant for a low-density region, in this paper we draw the attention to the performance of the correlation functionals.

To address the title issue, we carry out a systematic DFT study of the equilibrium binding energies and bond lengths of the methane dimer using 90 functionals. Methane is a nonpolar molecule with vanishing dipole and quadrupole moments. The first nonvanishing electrostatic interaction is the octopole−octopole interaction, and all higher-order interactions are weak and decay fast at large intermolecular separation. The dominant

† Part of the "Sheng Hsien Lin Festschrift".

* Corresponding author. E-mail: sdchao@spring.iam.ntu.edu.tw.

10.1021/jp074052n CCC: $37.00
Published on Web 08/24/2007

TABLE 1: Comparison of the Bond Lengths (in Å) Calculated with the 90 Exchange-Correlation Functionals Using the 6-311++G(3df,3pd) Basis Set[a]

	correlation functional									
exchange functional	VWN5	PL	TPSS	PBE	PW91	VWN	P86	VP86	LYP	HCTH
B88	U	U	U	U	U	U	U	U	U	**3.62**
HCTH	5.85	5.85	5.93	5.93	5.93	5.83	6.14	6.14	5.90	**3.92**
OPTX	5.20	5.20	5.24	5.23	5.24	4.93	5.30	5.30	4.83	**3.81**
MPW	4.77	4.77	4.84	4.84	4.83	4.73	4.69	4.69	4.26	**3.57**
TPSS	4.40	4.40	4.42	4.41	4.40	4.35	**4.03**	**4.03**	**3.98**	**3.52**
PBE	4.26	4.25	**4.08**	**4.06**	**4.04**	4.21	**3.72**	**3.72**	**3.79**	**3.53**
PW91	4.19	4.19	**4.05**	**4.04**	**3.99**	4.14	**3.72**	**3.73**	**3.80**	**3.52**
Slater	3.33	**3.99**	3.10	3.07	3.08	3.31	2.99	3.00	3.13	NA[b]
XAlpha	3.26	3.26	**3.54**	**3.52**	2.97	3.24	**3.49**	3.00	3.07	3.15

[a] As a reference, the MP2 bond length calculated at this basis set is 3.73 Å.[22] The better DFT results of errors within 10% as compared to the MP2 result are marked in boldface. [b] Not available

TABLE 2: Comparison of the Binding Energies (in kcal/mol) Calculated with the 90 Exchange-Correlation Functionals Using the 6-311++G(3df,3pd) Basis Set[a]

	correlation functional									
exchange functional	VWN5	PL	TPSS	PBE	PW91	VWN	P86	VP86	LYP	HCTH
B88	1.206	1.206	1.090	1.075	1.054	1.130	0.802	0.801	0.718	−1.749
HCTH	−0.007	−0.007	−0.003	−0.003	−0.004	−0.008	0.000	0.000	−0.006	−0.668
OPTX	−0.030	−0.030	−0.020	−0.020	−0.021	−0.032	−0.007	−0.006	−0.039	−1.582
MPW	−0.085	−0.085	−0.070	−0.070	−0.071	−0.096	−0.057	−0.056	−0.150	−2.559
TPSS	−0.087	−0.087	−0.074	−0.074	−0.077	−0.105	−0.118	−0.116	−0.250	−2.753
PBE	−0.149	−0.150	−0.157	−0.158	−0.167	−0.174	−0.358	−0.353	−0.457	−3.174
PW91	−0.358	−0.360	**−0.376**	**−0.379**	**−0.418**	**−0.387**	−0.577	−0.572	−0.669	−3.367
Slater	−1.173	−1.184	−2.330	−2.445	−2.483	−1.287	−3.436	−3.416	−2.884	NA[b]
XAlpha	−1.290	−1.302	−2.500	−2.634	−2.671	−1.415	−3.702	−3.640	−3.119	−5.838

[a] As a reference, the MP2 binding energy calculated at this basis set is −0.415 kcal/mol.[22] Positive values represent unbound dimer structures, and the energies are calculated at $R = 3.73$ Å. The better DFT results of errors within 10% as compared to the MP2 result are marked in boldface. [b] Not available

attraction for the methane dimer is thus due to the van der Waals force. Therefore, the calculation of van der Waals interactions of the methane dimer serves as a prototype study to investigate the various factors affecting the calculations of these interactions.

Theory and Calculations

In a previous study,[22] we found that for the methane dimer, a large part of the exchange−repulsion interactions can be calculated by the HF method. The calculation of electron correlation energies depends on the level of the correlation-corrected method, the size of the basis set, and the correction of the basis set superposition error (BSSE). It has been found that the MP2 results for the methane dimer are not too much different from those calculated by the much more expensive CCSD(T) as long as a large basis set has been used. The MP2 binding energy[22] is used as a reference value to calibrate the accuracy of current DFT calculations. Pople's medium size basis set, 6-311++G(3df, 3pd),[23] was used for all the calculations presented. This basis set has been proven accurate in determining the binding energy of the methane dimer up to 0.1 kcal/mol accuracy.[22] The basis set superposition error was corrected by the counterpoise (CP) method of Boys and Bernardi.[24]

All the DFT calculations were performed using the Gaussian 03 program package[25] on an AMD 250 computer cluster with distributed memory. The equilibrium geometry of a single methane molecule was first optimized at the MP2/6-31G* level of theory. To obtain the most stable intermolecular geometry, the methane dimer was modeled by first fixing the carbon−carbon (C−C) distance while letting the two monomers rotate freely. By approaching the monomers from the far side with several initial choices of mutual orientation, we found the minimum-energy conformation corresponds to the D_{3d} symmetry conformer. Subsequently the C−C distance was sampled in 0.1 Å steps for a large range of intermolecular separation (normally 3−9 Å). During the scan, we allow the individual methane molecule to be fully relaxed. This means that we do not fix the monomer geometry, and the methane molecule is not assumed to be rigid.

The density functionals used in the present work include the 90 combinations chosen among nine exchange (B88,[26] OPTX,[27] MPW,[28] PBE,[29] PW91,[30] TPSS,[31] Slater,[32] HCTH,[33] XAlpha[34]) and 10 correlation (TPSS,[31] PBE,[29] PW91,[30] P86,[35] HCTH,[33] VWN5,[36] PL,[37] VWN,[36] LYP[38]) functionals. We also consider several hybrid functionals of B971,[39] BB98,[40] BHandH,[41] O3LYP,[42] B3PW91,[43] PBE1PBE,[29] and MPW1PW91.[44] The chosen functionals are selective representations of the most commonly used density functionals for van der Waals interactions in current literature. Recent studies showed that the PW91PW91 functional could yield reasonable binding energy of the methane dimer interaction,[22] but the relative performance of the exchange and correlation functionals has not been systematically studied.

Results and Discussion

In Table 1, we show the bond lengths using the 90 exchange-correlation functionals, displayed as the row and the column items, respectively. Roughly, the bond lengths descend across the row and down the column. Compared with the MP2 result (3.73 Å), we find the PW91VP86 functional yields a value (3.73 Å) the same as the MP2 result. Table 2 presents the calculated binding energies using the 90 exchange-correlation functionals. These data are organized in a particular order, as shown in Table 2. In this order, the (negative) DFT potentials descend across the row and down the column. The results clearly demonstrate the relative performance of the exchange and the correlation functionals in the DFT calculations. By fixing the PW91 as the

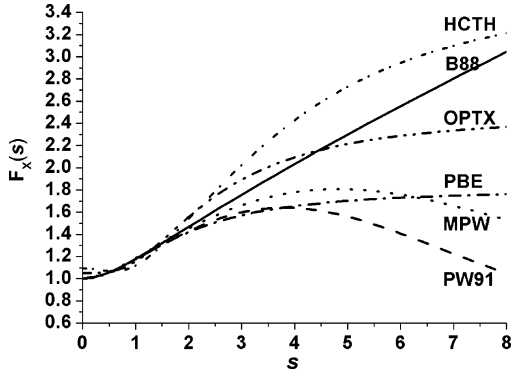

Figure 1. GGA exchange enhancement factor as a function of *s* for the B88, HCTH, OPTX, MPW, PBE, and PW91 exchange functionals.

exchange functional, for example, all correlation functionals yield bound potentials. On the other hand, by fixing the PW91 as the correlation functional, the varying exchange functionals much underestimate or overestimate the binding energy except the PW91 exchange functional. One of the combinations, PW91PW91, yields a binding energy (−0.418 kcal/mol) close to the MP2 result (−0.415 kcal/mol). Previous studies on van der Waals systems[45] have shown that the exchange functional plays an essential role in determining the binding energy, while the correlation part of a density functional does not significantly affect the DFT calculations. Our results are consistent with the former observation, while we see appreciable effects due to the choice of the correlation functional. To further analyze the results, we examine the large *s* behavior of the GGA enhancement factors at the asymptotically low-density region.

The performance of varying the GGA exchange functionals for a fixed correlation functional can be understood in terms of the behavior of the GGA enhancement factor $F_X(s)$ of the exchange functional for the large reduced density gradient region.[45] The exchange enhancement factor is defined by

$$F_X(s) = \frac{\epsilon_X^{\mathrm{GGA}}}{\epsilon_X^{\mathrm{LDA}}} \tag{1}$$

where $\epsilon_X^{\mathrm{GGA}}$ and $\epsilon_X^{\mathrm{LDA}}$ are the exchange potentials for the GGA and the LDA energy functionals, respectively. We plot the $F_X(s)$ versus *s* curve in Figure 1. We see in Figure 1 that the order of the magnitude of $F_X(s)$ at large *s* is B88 > OPTX > MPW > PBE > PW91. This order is essentially the order of the binding energies calculated by the corresponding functionals down the column in Table 2. This connection has been found in previous studies on van der Waals systems[45] and serves as a useful tool in analyzing the DFT calculations. In the present work, we verify and extend the utilities of previous conclusions. Notice that the HCTH functional is an outlier to the previous trend. This could be due to the fact that the original set up of using an HCTH exchange functional should always work with its correlation counterpart.[33]

On the other hand, the performance of varying the GGA correlation functionals for a fixed exchange functional has not been thoroughly studied before. In calculations for chemically bonded systems or hydrogen-bonded systems, the contribution of a correlation functional is often small. However, for low density and large *s*, the contribution of correlation energy becomes more significant.[29] In Table 2, we see that, for a fixed exchange functional, it may amount to a wide range of binding energies by varying the correlation functional. Because most GGA correlation functionals use the LDA correlation as an additive ingredient in the definition, to clearly show the nonlocal effect, an enhancement factor is defined by

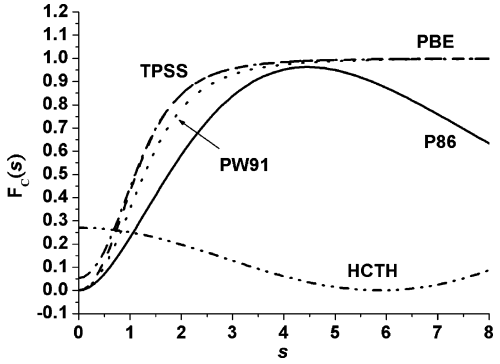

Figure 2. GGA correlation enhancement factor as a function of *s* for the TPSS, PBE, PW91, P86, and HCTH correlation functionals. Here $r_s = 10$.

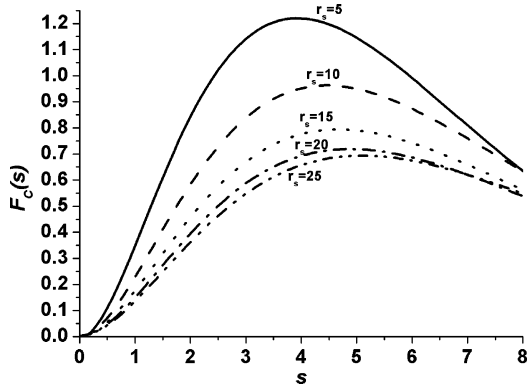

Figure 3. r_s dependence of the GGA correlation enhancement factor as a function of *s* for the P86 correlation functional.

$$F_C(s,r_s) = 1 - \frac{\epsilon_C^{\mathrm{GGA}}}{\epsilon_C^{\mathrm{LDA}}} \tag{2}$$

where $\epsilon_C^{\mathrm{GGA}}$ and $\epsilon_C^{\mathrm{LDA}}$ are the correlation potentials for the GGA and the LDA energy functionals, respectively. The correlation enhancement factor depends on *s* and r_s, where $r_s = (3/4\pi\rho)^{1/3}$ is the Wigner−Seitz radius. For van der Waals interactions, r_s falls in the range of 5−20. By fixing $r_s = 10$, we plot the enhancement factor $F_C(s)$ as a function of *s* in Figure 2. We see in Figure 2 that the order of the magnitude of $F_C(s)$ at medium *s* is TPSS > PBE > PW91 > P86 > HCTH. Interestingly, this order is essentially the order of the binding energies calculated by the corresponding functionals across the row in Table 2. These observations clearly show that the DFT potentials are correlated to the exchange and the correlation enhancement factors at the asymptotically low-density region. It requires the proper match of an exchange functional and a correlation functional to yield reasonable results. Most correlation functionals are not sensitive to the r_s for medium *s* range, except the P86 correlation functional. In Figure 3, we plot the r_s dependence of the correlation enhancement factor for the P86 functional as a function of *s*. We see that there is a significant effect of varying r_s on the P86 functional. Therefore, one has to be more careful in making conclusions with the P86 correlation functional.

Parts a−e of Figure 4 present the calculated potential curves by fixing five correlation functionals, respectively, and varying the exchange functions used in this paper. Figure 5 presents the potential curves using some hybrid functionals. We see that

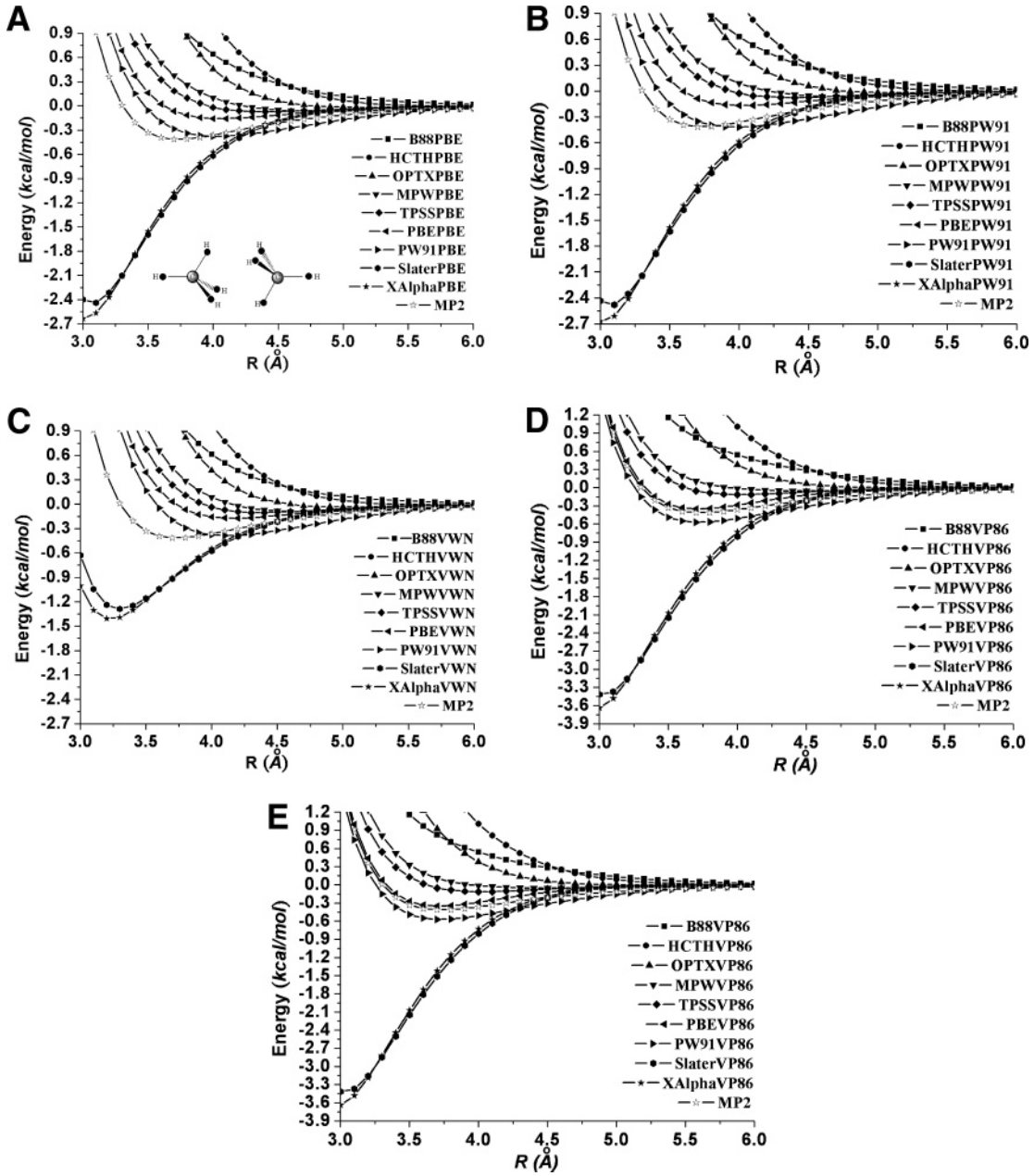

Figure 4. BSSE corrected potential curves with varying exchange functionals by fixing (a) PBE, (b) PW91, (c) VWN, (d) VP86, and (e) LYP correlation functionals, respectively. The MP2 potential curve is also shown as a reference.

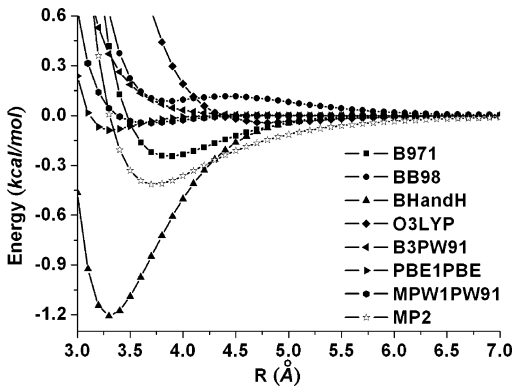

Figure 5. BSSE corrected potential curves selective using several hybrid functionals.

the DFT calculations generate a wide range of potential patterns. Some are purely repulsive (such as B88PBE), while others could be overbounded (such as SlaterVWN). There patterns have been found before and have often been termed "unsystematic". From our analysis, it is clear that some compensation among the respective exchange and correlation functions at the large *s* range of the enhancement factors must occur to yield reasonable potential well depth close to the MP2 result. For the methane case, PW91PW91 seems to achieve such appropriate compensation and thus yields a better result. Just exactly which combination should be used for a specific system is unknown a priori. Nevertheless, our Table 2 does show the interesting correlation between the calculated results and the chosen functionals and should provide a useful reference for choosing such a combination.

Next, we would like to discuss the asymptotic behaviors of some selective DFT potentials and compare them with those obtained from the MP2 reference potential. It is well-known that a DFT potential cannot be used to model the long-range tail of the van der Waals interaction. However, exactly how bad the situation is has not been systematically studied. Figure

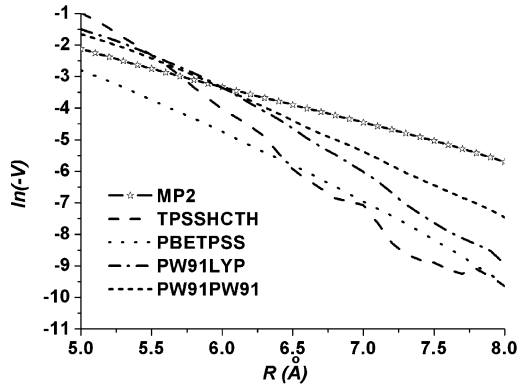

Figure 6. Asymptotic behavior of selective DFT potentials vs the MP2 potential via analysis of the long-range data.

6 displays the linear analysis of the potential curves by plotting $\ln(-V)$ versus $\ln(R^{-1})$, namely

$$\ln(-V) \propto \ln(R^{-6}) \tag{3}$$

where V is the (negative) potential energy by subtracting the HF potential (which is purely repulsive) from the DFT potential and R is the C−C distance. The data for $R > 5$ Å has been used to perform this analysis. Notice that the MP2 potential yields a reasonably straight line. Generally, DFT potentials yield erratic long-range behaviors. The deviation from the straight (MP2) line indicates the inefficacy of the DFT potentials. This verifies that DFT potentials cannot be used to model the dispersion interactions, in particular at long-range regions.[46]

To sum up this paper, we have studied the DFT potentials for van der Waals interactions of the methane dimer. Weak interactions of van der Waals systems have been widely studied and discussed in various contexts, and the DFT results were often termed "unsystematic". Definitely part of the reasons can be attributed to the error cancellation between the exchange and the correlation functionals. To study their relative performance, we analyze the exchange and the correlation enhancement factors in the asymptotically low-density region. Our objective is to make these results more "systematic" so that the calculated DFT potentials can be better understood. Similar to the exchange enhancement factor, the correlation enhancement factor, being useful for choosing a specific functional, should also be useful for constructing more exact functionals by "more constraint satisfaction with fewer fits".[47]

Acknowledgment. This work was supported by the National Science Council of Taiwan, ROC (NSC-95-2113-M-002-028-MY3, NSC-95-2120-M-002-006). We acknowledge the National Center for High-Performance Computing (NCHC) for providing computing resources. We would like to thank J. C. Jiang and M. Hayashi for useful discussions.

References and Notes

(1) Kipnis, A. Y.; Yavelov, B. E.; Rowlinson, J. S. *Van der Waals and Molecular Sciences*; Clarendon: New York, 1996.

(2) Jeffrey, G. A.; Saenger, W. *Hydrogen Bonding in Biological Structures*; Springer-Verlag: Berlin, 1991.

(3) Hobza, P.; Zahradnik, R. *Intermolecular Complexes: The Role of van der Waals Systems in Physical Chemistry and in the Biodisciplines*; Elsevier: New York, 1988.

(4) Margenau, H. *Rev. Mod. Phys.* **1939**, *11*, 1.

(5) van der Avoird, A.; Wormer, P. E. S.; Moszynski, R. *Chem. Rev.* **1994**, *94*, 1931.

(6) Rappe, A. K.; Bernstein, E. R. *J. Phys. Chem. A* **2000**, *104*, 6117.

(7) Chalasinski, G.; Szczesniak, M. M. *Chem. Rev.* **2000**, *100*, 4227.

(8) Wheatley, R. J.; Tulegenov, A. S.; Bichoutskaia, E. *Int. Rev. Phys. Chem.* **2004**, *23*, 151.

(9) Zhao, Y.; Truhlar, D. G. *J. Chem. Theory Comput.* **2005**, *1*, 415.

(10) Moller, C.; Plesset, M. S. *Phys. Rev.* **1934**, *46*, 618.

(11) Pople, J. A.; Head-Gordon, M.; Raghavachari, K. *J. Chem. Phys.* **1987**, *87*, 5968.

(12) Dykstra, C. E., Frenking, G., Kim, K. S., Scuseria, G. E., Eds. *Theory and Applications of Computational Chemistry: The First Forty Years*; Elsevier: Amsterdam, 2005.

(13) Dreizer, R. M.; Gross, E. K. U. *Density Functional Theory*; Springer: Berlin, 1990.

(14) Grimme, S. *J. Comput. Chem.* **2004**, *25*, 1463.

(15) Cybulski, S. M.; Seversen, C. E. *J. Chem. Phys.* **2005**, *122*, 014117.

(16) Zhao, Y.; Truhlar, D. G. *J. Phys. Chem. A* **2006**, *110*, 5121.

(17) Becke, A. D. *J. Chem. Phys.* **2000**, *112*, 4020.

(18) Toulouse, J.; Colonna, F.; Savin, A. *J. Chem. Phys.* **2005**, *122*, 014110.

(19) Handy, N. C.; Cohen, A. J. *Mol. Phys.* **2001**, *99*, 403.

(20) Jones, R. O.; Gunnarsson, O. *Phys. Rev. Lett.* **1985**, *55*, 107.

(21) Perdew, J. P.; Wang, Y. *Phys. Rev. B* **1986**, *3*, 8800.

(22) Li, A. H. T.; Chao, S. D. *J. Chem. Phys.* **2006**, *125*, 094312.

(23) Krishnan, R.; Binkley, J. S.; Seeger, R.; Pople, J. A. *J. Chem. Phys.* **1980**, *72*, 650.

(24) Boys, S. F.; Bernardi, F. *Mol. Phys.* **1970**, *19*, 553.

(25) Frisch, M. J.; Trucks, G. W.; Schlegel, H. B.; Scuseria, G. E.; Robb, M. A.; Cheeseman, J. R.; Montgomery, J. A., Jr.; Vreven, T.; Kudin, K. N.; Burant, J. C.; Millam, J. M.; Iyengar, S. S.; Tomasi, J.; Barone, V.; Mennucci, B.; Cossi, M.; Scalmani, G.; Rega, N.; Petersson, G. A.; Nakatsuji, H.; Hada, M.; Ehara, M.; Toyota, K.; Fukuda, R.; Hasegawa, J.; Ishida, M.; Nakajima, T.; Honda, Y.; Kitao, O.; Nakai, H.; Klene, M.; Li, X.; Knox, J. E.; Hratchian, H. P.; Cross, J. B.; Bakken, V.; Adamo, C.; Jaramillo, J.; Gomperts, R.; Stratmann, R. E.; Yazyev, O.; Austin, A. J.; Cammi, R.; Pomelli, C.; Ochterski, J. W.; Ayala, P. Y.; Morokuma, K.; Voth, G. A.; Salvador, P.; Dannenberg, J. J.; Zakrzewski, V. G.; Dapprich, S.; Daniels, A. D.; Strain, M. C.; Farkas, O.; Malick, D. K.; Rabuck, A. D.; Raghavachari, K.; Foresman, J. B.; Ortiz, J. V.; Cui, Q.; Baboul, A. G.; Clifford, S.; Cioslowski, J.; Stefanov, B. B.; Liu, G.; Liashenko, A.; Piskorz, P.; Komaromi, I.; Martin, R. L.; Fox, D. J.; Keith, T.; Al-Laham, M. A.; Peng, C. Y.; Nanayakkara, A.; Challacombe, M.; Gill, P. M. W.; Johnson, B.; Chen, W.; Wong, M. W.; Gonzalez, C.; Pople, J. A. *Gaussian 03*, revision C.02; Gaussian, Inc.: Wallingford, CT, 2004.

(26) Becke, A. D. *Phys. Rev. A* **1988**, *38*, 3098.

(27) Handy, N. C.; Cohen, A. J. *Mol. Phys.* **2001**, *99*, 403.

(28) Adamo, C.; Barone, V. *J. Chem. Phys.* **1998**, *108*, 664.

(29) Perdew, J. P.; Burke, K.; Ernzerhof, M. *Phys. Rev. Lett.* **1996**, *77*, 3865.

(30) Burke, K.; Perdew, J. P.; Wang, Y. In *Electronic Density Functional Theory: Recent Progress and New Directions*; Ed. Dobson, J. F., Vignale, G., Das, M. P., Eds.; Plenum Publishing: New York, 1998.

(31) Tao, J.; Perdew, J. P.; Staroverov, V. N.; Scuseria, G. E. *Phys. Rev. Lett.* **2003**, *91*, 146401.

(32) Kohn, W.; Sham, L. J. *Phys. Rev.* **1965**, *140*, A1133.

(33) Boese, A. D.; Handy, N. C. *J. Chem. Phys.* **114**, 5497; see also the supporting material: EPAPS document no. 2001, E-JCPA6-114-301111.

(34) Slater, J. C. *Quantum Theory of Molecular and Solids. Vol. 4: The Self-Consistent Field for Molecular and Solids*; McGraw-Hill: New York, 1974.

(35) Perdew, J. P. *Phys. Rev. B* **1986**, *33*, 8822.

(36) Vosko, S. H.; Wilk, L.; Nusair, M. *Can. J. Phys.* **1980**, *58*, 1200.

(37) Perdew, J. P.; Zunger, A. *Phys. Rev. B* **1981**, *23*, 5048.

(38) Lee, C.; Yang, W.; Parr, R. G. *Phys. Rev. B* **1988**, *37*, 785.

(39) Hamprecht, F. A.; Cohen, A. J.; Tozer, D. J.; Handy, N. C. *J. Chem. Phys.* **1998**, *109*, 6264.

(40) Schmider, H. L.; Becke, A. D. *J. Chem. Phys.* **1998**, *108*, 9624.

(41) Becke, A. D. *J. Chem. Phys.* **1993**, *98*, 1372.

(42) Cohen, A. J.; Handy, N. C. *Mol. Phys.* **2001**, *99*, 607.

(43) Becke, A. D. *J. Chem. Phys.* **1993**, *98*, 5648.

(44) Adamo, C.; Barone, V. *J. Chem. Phys.* **1998**, *108*, 664.

(45) Zhang, Y.; Pan, W.; Yang, W. *J. Chem. Phys.* **1997**, *107*, 7921.

(46) Li, A. H.-T.; Chao, S. D. *Phys. Rev. A* **2006**, *73*, 016701.

(47) Perdew, J. P.; Ruzsinsky, A.; Tau, J.; Staroverov, V. N.; Scuseria, G. E.; Csonka, G. I. *J. Chem. Phys.* **2005**, *123*, 062201.